Journal of Analytical Science and Technology

RESEARCH ARTICLE

Open Access

Nail fold capillaroscopy as a potential tool to evaluate breast tumor

Minsuk Kim[1*]

Abstract

It is necessary to verify whether nail fold capillaroscopy can be utilized for the early detection of breast cancer. To establish this technology, an animal model was developed, utilizing mice for nail fold observations. Nail fold capillaroscopy revealed a human-like anatomical pattern and facilitated the observation of cellular movement within blood vessels. Injection of MCF-7 or mammary fibroblasts in mice allowed the observation of cellular vibrations using motion microscopy from nail fold. We have named this technology 'capillary cell motion microscopy.' Intriguingly, we were able to identify distinct cellular vibrations in the MCF-7 group. Moreover, evaluating its effectiveness in mice with chemically induced cancer revealed higher sensitivity (81%-85%) compared to conventional methods (45%-68%). Capillary cell motion microscopy, operating at 0.5–1.5 Hz, provided clear distinction of tumor cells and demonstrated potential applicability in human subjects. While condition adjustments may be necessary, this method holds promise for noninvasive breast cancer detection through nail fold observations.

Keywords Microfluidic system, Motion microscopy, Breast tumor, Computational tool, Vibration

Introduction

Circulating tumor cells (CTCs) are cells shed from a primary tumor and circulate in the bloodstream during cancer progression (Lin et al. 2021). Therefore, they may act as circulating biomarkers that enable prediction, diagnosis, and treatment assessment (Tiberio et al. 2023). Various techniques have been utilized and applied for the detection of CTCs (Bankó et al. 2019). These techniques comprise density-based separation, microfiltration, microfluidic sorting, immune magnetic affinity, or combination of these methods (Bankó et al. 2019). However, these methods commonly share the inconvenience of requiring a significant amount of blood (Huang et al. 2023; Qiu et al. 2018).

*Correspondence:
Minsuk Kim
ms@ewha.ac.kr
[1] Department of Pharmacology, Inflammation-Cancer Microenvironment Research Center, College of Medicine, Ewha Womans University, Magokdong-Ro 2-Gil, Gangseogu, Seoul 07804, Republic of Korea

It is possible to noninvasively observe blood cells through the human eye and nail fold (McKay et al. 2020; Li et al. 2023). In particular, the capillaries in the nail fold are more easily observable for continuous monitoring compared to the eye. The skin at the fingertips is densely populated with capillaries, allowing for the observation of the circulation of blood cells (Baran et al. 2015). Capillary imaging is achieved by positioning the objective lens perpendicular to the nail fold and selecting the magnification for capturing images without compressing the skin. Nowadays, there are capillary observation devices that can be easily attached to smartphones, enabling real-time diagnostics even in a home setting (Patterson et al. 2020).

Previously, we have developed a technology to detect the vibrations of tumor cells from blood (Kim, Ahn, Kim, Park, Yoon, Park, Moon, Ryu, Kang, et al. 2020). The principle involves amplifying specific frequency signals of subtle movements that can be stored in the pixels of a digital camera (Adiv 1985; Hurlburt and Jaffey 2015; Sellon et al. 2015; Wadhwa et al. 2017). Spatial local phase information was combined in different sub-bands

of frames for each pixel at location (x, y), time t, scale r, and orientation θ using squares objective function, $\underset{u,v}{\operatorname{argmin}} \sum_i A_{ri,i}^2 \left[\left(\frac{ri,i}{x}, \frac{ri,i}{y} \right)(u,v) - r_{i,i} \right]^2$ (Wadhwa et al. 2017). There have been studies conducted on using nail fold capillaroscopy for cancer diagnosis (Gollins and de Berker. 2021). However, morphological changes in the nail fold can also be found in various diseases such as chronic bronchitis, inflammatory bowel disease, rheumatoid arthritis, congestive heart failure, and hypothyroidism. The exact mechanisms behind these phenomena have not yet been elucidated. Therefore, nail fold capillaroscopy alone remains a premature technology for cancer diagnosis. Nonetheless, nail fold capillaroscopy holds potential for providing disease information without the need for blood sampling. There have been developments in using smartphones for cancer detection through photoelectrochemical immunoassays and biomineral probes for detecting cancer biomarkers in urine (Zeng et al. 2022; Yu et al. 2023). However, since cancer-specific markers may exist in small amounts or not be expressed on the surface of cancer cells, there is a need to develop methods that do not rely on cancer-specific markers. Motion microscopy technology offers a solution by detecting unique vibration signatures caused by Catenin Delta 1 and Actin Gamma 1, which are present in normal cells as well (Kim et al. 2020). This method allows for the detection of cancer cells without relying on cancer-specific biomarkers. Therefore, we aim to combine these two technologies to explore whether noninvasive tumor cell discrimination is possible in the nail fold. To start with this, we amplified the capillary images of mouse nail folds using a motion microscope.

Materials and methods

Animal treatment

All mice were in C57BL/6 (RRID: 2,159,769) background and purchased from Charles River. All experiments using animals were approved and performed by the Ewha Womans University Animal Care Committee (Guide for the care and use of laboratory animals; IRB number: ESM14-0260). Ten female mice were each given by subcutaneous injection of MCF-7 cells or human mammary fibroblasts (1×10^6 cells in 100 mL phosphate buffered saline). For carcinogenesis model, seventeen female mice were each given weekly 1 mg doses of 7,12-Dimethylbenzathracene (DMBA) in 0.2 ml of sesame oil by oral gavage for six weeks and were implanted with 30 mg pellets of compressed medroxyprogesterone acetate (MPA) subcutaneously beginning at 5 weeks of age.

Cell culture

Human breast cancer cell lines, MCF-7 (ATCC; RRID: CVCL_0031), was maintained in Dulbecco's MEM (11,885, Gibco, USA) with 10% bovine serum (16,000,044, Gibco, USA), and human mammary fibroblast was obtained from cell biologics (H-6071, USA) and maintained in fibroblast medium (Cell Biologics, M2267, USA) with 10% fetal bovine serum (16,000,044, Gibco, USA) at 37 ℃ under an atmosphere of 95% O_2 and 5% CO_2.

Real-time PCR

RNA levels of *ERBB2* (Hs01001580_m1, Life Technology) were determined using primer/probe set from Life Technology. Real-time PCR was performed with TaqMan PCR Mix on an ABI PCR System 7000 (Applied Biosystems, USA). PCR conditions were 50 °C for 2 min and 95 °C for 10 min, followed by 40 cycles of 95 °C for 15 s and 60 °C for 1 min. For each experimental sample, the relative abundance value was normalized to the value derived from *ACTB* (Hs03023943_g1, Life Technology) as housekeeping control gene. Relative mRNA levels were quantified using the comparative $2^{-\Delta\Delta CT}$ method.

Nail fold capillaroscopy

Nail fold capillaroscopy was performed with a capillaroscope model JH-1004C with a total magnification of 380 to obtain video files recorded. Nail fold capillaroscopy was performed at room temperature on the front and hind limbs of the specimen. The excess hairs near the nail fold were trimmed, and immersion oil was applied to the nail fold.

Experimental procedures of motion microscope and microfluidic device

MCF-7 or human primary mammary fibroblasts were introduced to microfluidic device at a flow rate of 22 μm/s, and images were recorded through microscope at 1024 × 576 pixels and 900 frames per second. The recorded images were uploaded to lambda vue (https://lambda.qrilab.com/site/), and magnification was done with amplification ratio of 35 and wavelength from 0.1 Hz to 10 Hz. Microfluidic devices (Microfit, South Korea) were placed on the stage of the microscope, and the fluid flow was controlled by individual syringe pumps (BS-9000–12, Braintree scientific, USA).

Quantification of cellular trail intensity

The obtained images were subtracted through the rolling ball radius method, and cellular trails were individually selected. The area of histograms was quantified by

ImageJ (Java-based image processing and analysis software). Data were acquired as arbitrary area values.

Fluorescence microscope

Briefly, cells were placed in 10% formalin for 3 h and incubated with antisera against FITC-conjugated *ERBB2* (1:400; ab134182, Abcam, USA). After washing with PBS, cells were visualized using Zeiss LSM 510 confocal microscope (Carl Zeiss, German).

Statistical analysis

Values are means ± SE. The significance of differences was determined by a one-way ANOVA followed by a Bonferroni post hoc analysis where appropriate. Differences were considered significant when $P < 0.05$.

Results and discussion

Detection for tumor cells using nail fold capillaroscopy

Although nail fold capillaroscopy is not commonly associated with breast cancer detection, innovative approaches can be explored to leverage this technique for early diagnosis. To develop technology for detecting cancer cells in nail fold images, an animal model was required. There have been reports that guinea pigs are an animal model in which nail pods similar to those of humans can be observed (Mandujano and Golubov

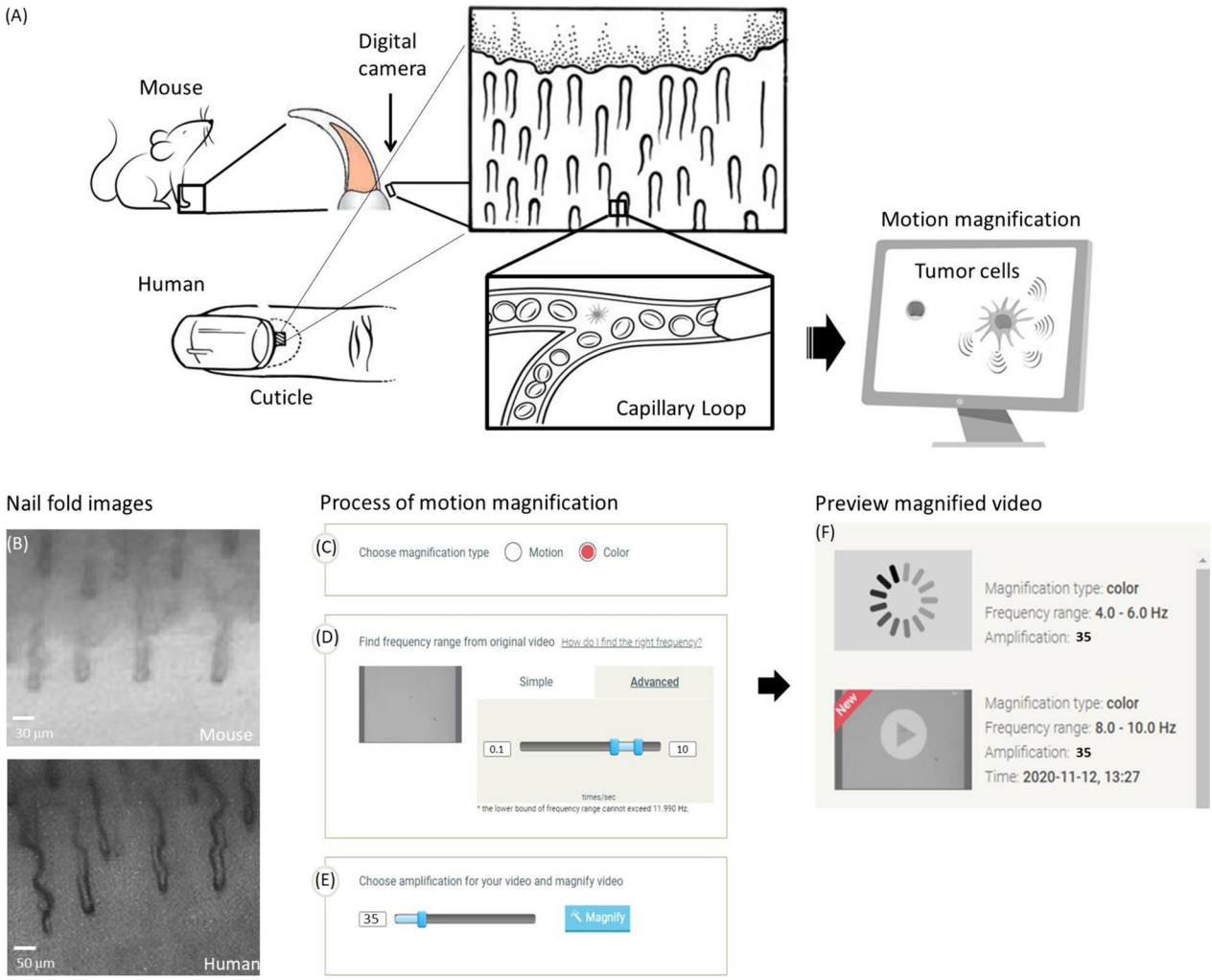

Fig. 1 Tumor cells detection from nail fold capillaries. **A** Schemata of the experimental setup of nail fold capillaroscopy and motion microscope. The excess animal hairs near the nail fold were trimmed, and immersion oil was applied to the nail fold. **B** Images of nail folds in animals and humans were recorded through capillaroscopy. Video recording files were obtained from the microscope at 1024 × 576 pixels at 600 frames per second. Micromotions were amplified by video using spatial local phase. **C** The obtained videos were entered at lambda vue, and color modes were selected in magnification type. After setting the wavelengths between 0.1 and 10 Hz (**D**), cellular vibrations were amplified 35 times (**E**) and magnified images obtained (**F**)

2022). To investigate whether nail fold capillaroscopy is feasible in mice as well, the excess hair was trimmed, and immersion oil was applied, and observed the nail folds. Capillaries were observed through nail fold capillaroscopy at a magnification of 300 times, and images were captured at a resolution of 1024×576 pixels with 800 frames per second (Fig. 1A). The anatomical pattern closely resembled the human nail fold, featuring a U-shape or a hairpin-like configuration (Fig. 1B). Additionally, it allowed for the observation of cellular movement within the blood vessels. Additionally, we observed the vibration of cancer cells from the nail fold images of mice. The cellular vibrations were enhanced using a motion microscope, with specific settings in color mode and magnification type as illustrated in Fig. 1C. The wavelength ranged from 0.1 to 10 Hz (Fig. 1D), and the amplification rate was set at 35 times (Fig. 1E). The resultant modified images were acquired through the aforementioned process, as depicted in Fig. 1F.

Vibration of breast tumor cells according to wavelengths

Before injecting breast cancer cells into the animal model, we confirmed the ability to detect the vibrations of the breast cancer cells. It has been reported that vibrations are observed in breast tumor cells at 0.5 to 1.5 Hz (Kim, Ahn, Kim, Park, Yoon, Park, Moon, Ryu, Lee Kang, et al. 2020). Here, 1 Hz corresponds to 60 invisible repetitive movements over 60 s. As expected, the vibrations were prominently observed in MCF-7 cells, but not human mammary fibroblasts (Fig. 2A and B).

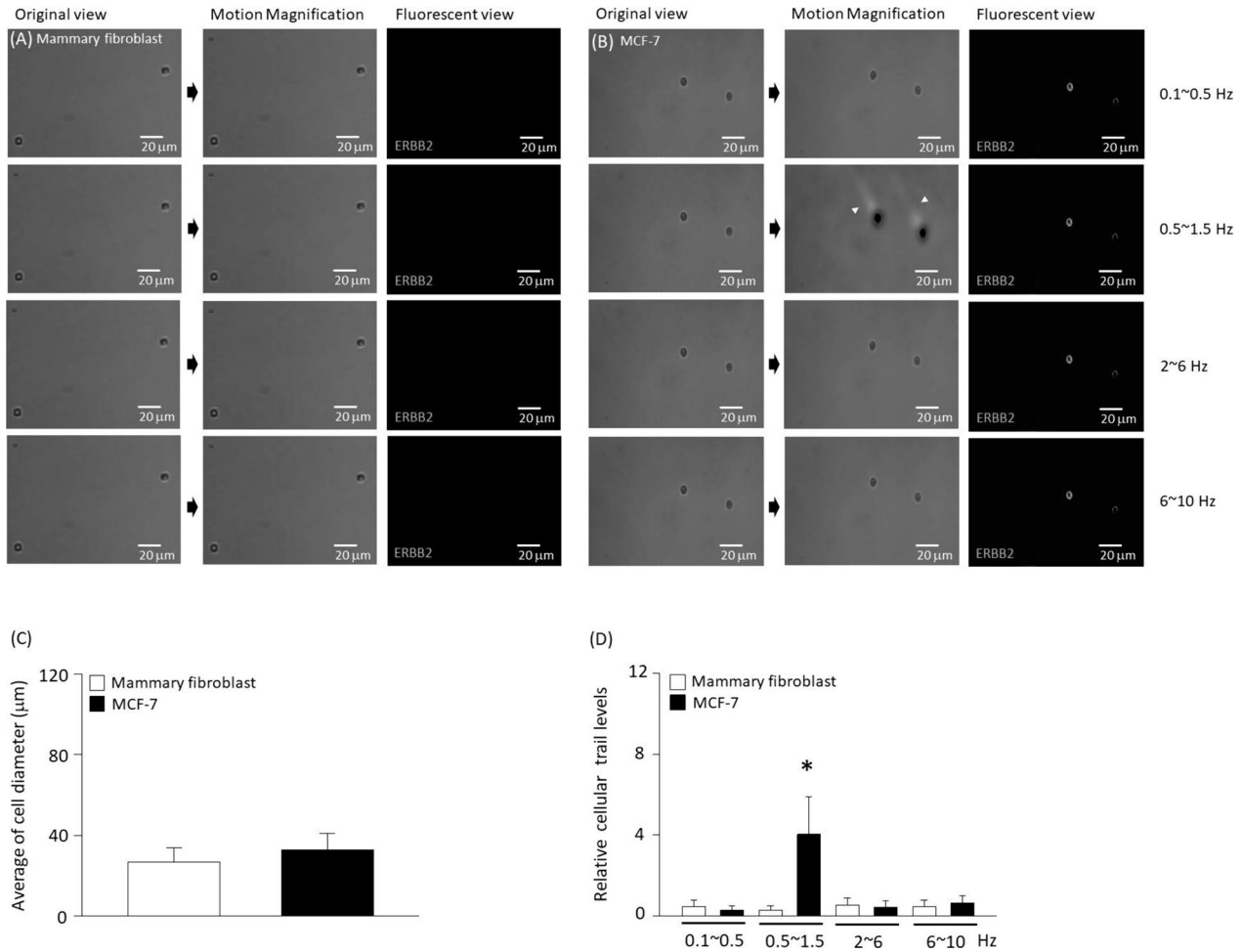

Fig. 2 Motion magnified video revealed cellular vibration. The images of cellular vibration of human mammary fibroblast (**A**) or MCF-7 (**B**) were converted by a motion microscope at 0.1 Hz to 10 Hz. MCF-7 showed distinct cellular trails (arrow heads) between 0.5 and 1.5 Hz. Cells were immunostained with *ERBB2* antibody and detected using fluorescence microscopy. **C** Diameters of human mammary fibroblast or MCF-7. **D** Intensity levels of cellular trails in motion magnified videos between 0.5 and 1.5 Hz. Results are the means ± SE of 6 experiments in each group. *Significantly different from motion magnified videos at 0.1 Hz to 0.5 Hz, $P < 0.05$

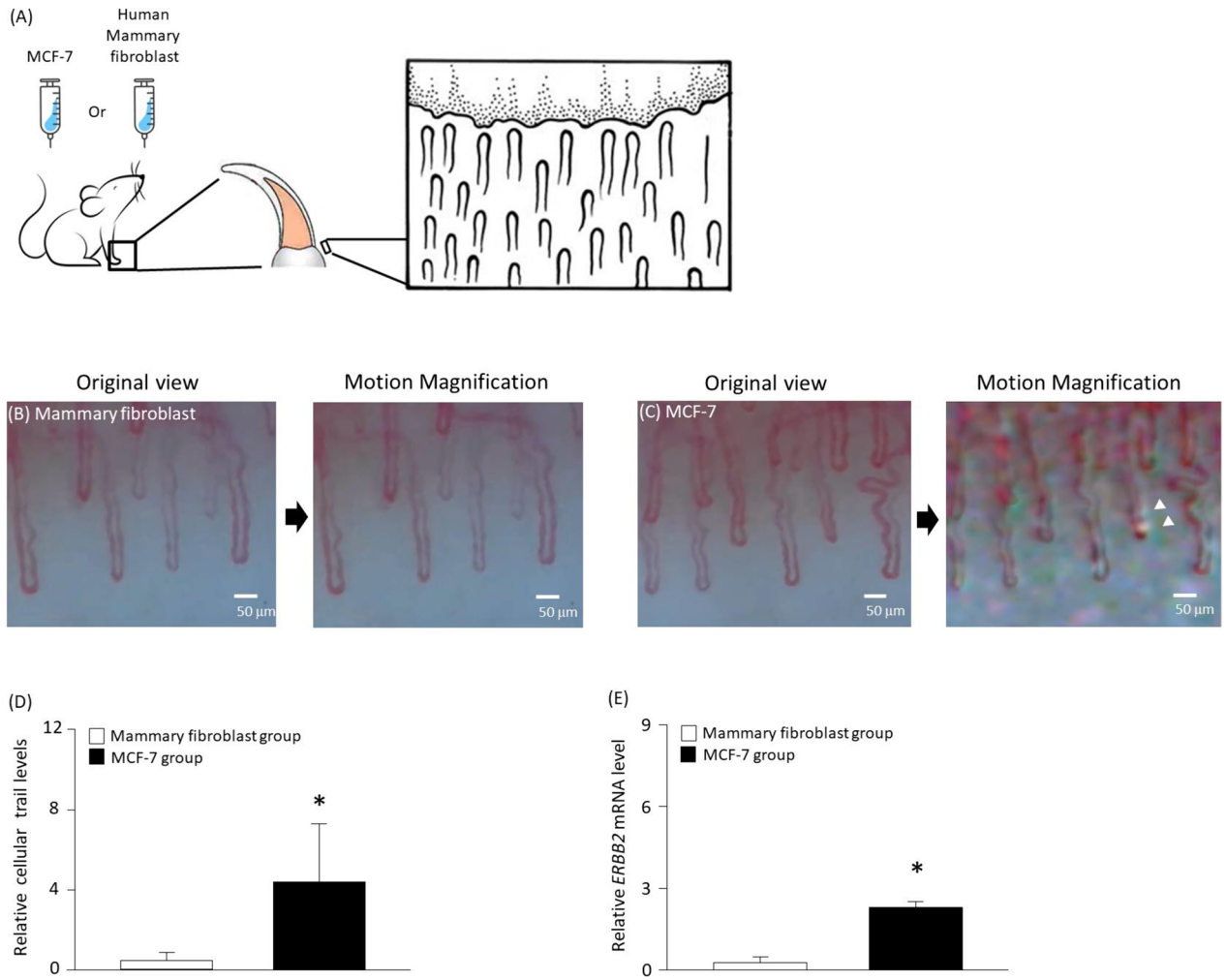

Fig. 3 Tumor vibration in mouse nail folds. **A** Beginning at 5 weeks of age, female mice were given subcutaneously mammary fibroblasts or MCF-7 cells for 2 weeks. **B** and **C** The vibrations in the obtained nail fold images were amplified between 0.5 and 1.5 Hz. MCF-7-treated group showed distinct cellular trails (arrow heads). **D** Intensity levels of cellular trails using motion microscopy. **E** Real-time PCR was performed using mRNA from blood cells to detect *ERBB2*. Results are the means ± SE of 6 experiments in each group. *Significantly different from mammary fibroblast-treated group, $P < 0.05$

Additionally, ERBB2, a positive marker for breast cancer cells, was prominently stained with fluorescence in MCF-7 (Klocker and Suppan 2020). There was no notable difference in the size of MCF-7 or human mammary fibroblasts (Fig. 2C). Under the discovered conditions, it was possible to distinguish tumor cells from mammary fibroblasts regardless of their size. (Fig. 2C and D).

Capturing vibrations of breast cancer cells in mouse nail folds

MCF-7 or mammary fibroblasts were injected into mouse, and images of nail capillaries were captured and magnified at a wavelength ranging from 0.1 to 1.5 Hz (Fig. 3A). Cellular vibrations were not found in the mouse group administered mammary fibroblast (Fig. 3B). However, the vibrations were observed in the nail folds of the mouse group administered MCF-7 cells (Fig. 3C and D). A relatively high level of *ERBB2* was detected in the blood of the group administered MCF-7, indicating that the tumor cells were properly administered to the animals (Fig. 3E). We referred to this observation method as capillary cell motion microscopy.

Capillary cell motion microscopy increases sensitivity of detecting breast cancer

The effectiveness of capillary cell motion microscopy was also investigated in mice that developed cancer caused by the chemical substance of DMBA (Fig. 4A). A relatively

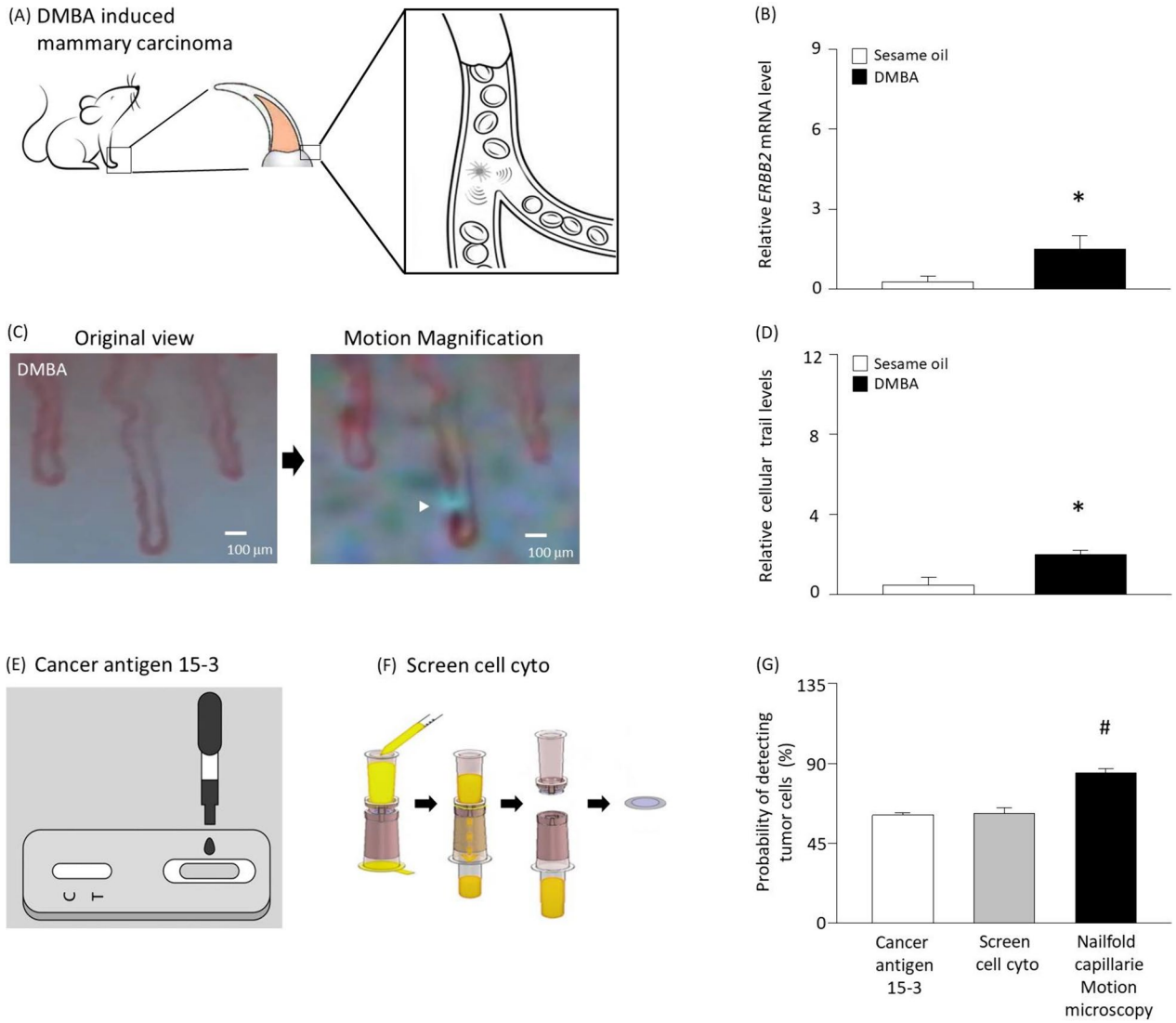

Fig. 4 Detecting tumor cells using capillary cell motion microscopy. **A** Beginning at 5 weeks of age, female mice were given 1 mg of DMBA by oral gavage and 30 mg of subcutaneous pellets of MPA for 6 weeks. **B** Real-time PCR was performed using mRNA from blood cells to detect *ERBB2*. **C** DMBA-treated group showed distinct cellular trails (arrow heads). **D** Intensity levels of cellular trails using motion microscopy. **E**–**F** Schemata of the experimental setup to detect breast tumor using cancer antigen 15–3 or size-based filtration system (screen cell cyto). Cells excluding red blood cells were separated by centrifugation at 500 × g using the Red Blood Cell Lysis Buffer kit (Roche, 11,814,389,001) and used for Screen cell cyto analysis. **G** In detecting tumor cells, cancer antigen 15–3 and screen cell cyto were compared with capillary cell motion microscopy. Results are the means ± SE of 6 experiments in each group. *Significantly different from treatment of sesame oil, $P < 0.05$. #Significantly different from cancer antigen 15–3, $P < 0.05$

high level of *ERBB2* was detected in the blood of the DMBA-treated group, indicating that the tumor cells were circulating in capillaries (Fig. 4B). Cellular vibration was also observed in the nail folds of mice with the chemical carcinogenesis (Fig. 4C and D). To examine the performance of our capillary motion microscopy with other techniques, we compared it with cancer antigen 15–3 or screen cell cyto (Fig. 4E and F) (Fakhari et al. 2019; Desitter et al. 2011). The cancer antigen 15–3 or screen cell cyto detection methods yielded a sensitivity of 45%–68%, whereas capillary motion microscopy method detected tumor cells with a sensitivity of 81%-85% (Fig. 4G). Overall, tumor cells were clearly distinguishable using the capillary motion microscopy under condition of 0.5–1.5 Hz. Furthermore, although adjustment of conditions is inevitable, it shows the possibility of determining the presence or absence of the tumor cells from a person's nail fold.

Conclusion

The purpose of this experiment is to develop a diagnostic method for breast tumor cells through the visualization of microscopic vibrations. Recently, methods utilizing photoelectrochemical immunoassays and biomineral probes have been developed. However, these methods require specific amounts of blood and face difficulties in detecting cancers with minimal expression of specific markers. In contrast, a method that involves continuous video recording from fingernail folds to detect the presence of tumor cells does not overlap with the existing detection spectrum. Moreover, it offers the convenience of not requiring blood samples and demonstrates high sensitivity. Therefore, we provide a new tool for breast tumor detection with potential clinical utility.

Acknowledgements
We thank Minjeong Kim (Ewha medical student) for helping to culture tumor cells.

Author contributions
MK designed and performed experiments, analyzed data, prepared figures, and wrote manuscript.

Funding
This work was supported by the National Research Foundation of Korea (NRF) grant (2020R1A5A2019210 and 2019R1C1C1003384) funded by the Korean government (MSIT) and Ewha Womans University Research Grant of 2023.

Availability of data and materials
All data supporting the findings of this study are available within the paper.

Declarations

Competing interests
No conflict of interests is declared.

Received: 21 March 2024 Accepted: 2 June 2024
Published online: 10 June 2024

References

Adiv G. Determining three-dimensional motion and structure from optical flow generated by several moving objects. IEEE Trans Pattern Anal Mach Intell. 1985;7(4):384–401.
Bankó P, Lee SY, Nagygyörgy V, Zrínyi M, Chae CH, Cho DH, Telekes A. Technologies for circulating tumor cell separation from whole blood. J Hematol Oncol. 2019;12(1):48–68.
Baran U, Shi L, Wang RKK. Capillary blood flow imaging within human finger cuticle using optical microangiography. J Biophotonics. 2015;8(1–2):46–51.
Desitter I, Guerrouahen BS, Benali-Furet N, Wechsler J, Janne PA, Kuang Y, Yanagita M, Wang L, Berkowitz JA, Distel RJ, Cayre YE. A new device for rapid isolation by size and characterization of rare circulating tumor cells. Anticancer Res. 2011;31(2):427–41.
Fakhari A, Gharepapagh E, Dabiri S, Gilani N. Correlation of cancer antigen 15–3 (CA15-3) serum level and bony metastases in breast cancer patients. Med J Islam Repub Iran. 2019;33:142–8.
Gollins CE, de Berker D. Nails in systemic disease. Clin Med. 2021;21:166–9.
Huang X, Lin Q, Gong H, Lu L, Wei Q, Tang D. Bio-inspired nanozyme with ultra-thin Fe-Bi(2)O(2)S nanosheets for in-situ amplified photoelectrochemical immunoassay of cancer-related protein. Anal Chim Acta. 2023;1252:341058–68.
Hurlburt N, Jaffey S. A spectral optical flow method for determining velocities from digital imagery. Earth Sci Inform. 2015;8:959–65.
Kim H, Ahn YH, Kim BS, Park S, Yoon JC, Park J, Moon CM, Ryu DR, Lee Kang J, Choi JH, Park EM, Lee KE, Woo M, Kim M. Motion microscopy for label-free detection of circulating breast tumor cells. Biosens Bioelectron. 2020;158:112131–9.
Klocker EV, Suppan C. Biomarkers in Her2- positive disease. Breast Care (basel). 2020;15(6):586–93.
Li JN, Wang DY, Pottenburgh J, Bower AJ, Asanad S, Lai EW, Simon C, Im L, Huryn LA, Tao Y, Tam J, Saeedi OJ. Visualization of erythrocyte stasis in the living human eye in health and disease. Iscience. 2023;26(1):105755–72.
Lin DF, Shen LS, Luo M, Zhang K, Li JF, Yang Q, Zhu FF, Zhou D, Zheng S, Chen YD, Zhou JJ. Circulating tumor cells: biology and clinical significance. Signal Transduct Target Ther. 2021;6(1):404–28.
Mandujano A, Golubov M. Animal models of systemic sclerosis: using nailfold capillaroscopy as a potential tool to evaluate microcirculation and microangiopathy: a narrative review. Life (basel). 2022;12(5):703–22.
McKay GN, Mohan N, Butterworth I, Bourquard A, Sánchez-Ferro A, Castro-González C, Durr NJ. Visualization of blood cell contrast in nailfold capillaries with high-speed reverse lens mobile phone microscopy. Biomed Opt Express. 2020;11(4):2268–76.
Patterson K, Walker J, Roberts-Thomson P. Nailfold capillaroscopy using smartphone technology. Intern Med J. 2020;50:17–8.
Qiu Z, Shu J, Tang D. Near-infrared-to-ultraviolet light-mediated photoelectrochemical aptasensing platform for cancer biomarker based on core-shell NaYF(4):Yb, Tm@TiO(2) upconversion microrods. Anal Chem. 2018;90:1021–8.
Sellon JB, Farrahi S, Ghaffari R, Freeman DM. Longitudinal spread of mechanical excitation through tectorial membrane traveling waves. Proc Natl Acad Sci U S A. 2015;112(42):12968–73.
Tiberio P, Gaudio M, Belloni S, Pindilli S, Benvenuti C, Jacobs F, Saltalamacchia G, Zambelli A, Santoro A, De Sanctis R. Unlocking the potential of circulating miRNAs in the breast cancer neoadjuvant setting: a systematic review and meta-analysis. Cancers. 2023;15(13):3424–48.
Wadhwa N, Chen JG, Sellon JB, Wei D, Rubinstein M, Ghaffari R, Freeman DM, Buyukozturk O, Wang P, Sun S, Kang SH, Bertoldi K, Durand F, Freeman WT. Motion microscopy for visualizing and quantifying small motions. Proc Natl Acad Sci U S A. 2017;114(44):11639–44.
Zeng R, Li Y, Li Y, Wan Q, Huang Z, Qiu Z, Tang D. Smartphone-based photoelectrochemical immunoassay with Co(9)S(8)@ZnIn(2)S(4) for point-of-care diagnosis of breast cancer biomarker. Research. 2022;2:9831521–31.

Publisher's Note